Aluminum K-XANES spectra in minerals as a source of information on their local atomic structure

1998 J. Phys.: Condens. Matter 10 5463

(http://iopscience.iop.org/0953-8984/10/24/022)

J. Phys.: Condens. Matter **10** (1998) 5463–5473. Printed in the UK PII: S0953-8984(98)90482-9

Aluminum K-XANES spectra in minerals as a source of information on their local atomic structure

L A Bugaev†‖, Ph Ildefonse‡, A-M Flank§, A P Sokolenko† and H V Dmitrienko†

† Department of Physics, Rostov University, Zorge street 5, Rostov-on-Don 344090, Russia
‡ Laboratoire de Mineralogie–Cristallographie, UA CNRS 09, Universités Paris 6 et 7, and IPGP, 4 place Jussieu, 75252 Paris Cédex 05, France
§ LURE, CNRS/CEA/MEN, Batiment 209D, 91405 Orsay, France

Received 7 January 1998, in final form 17 March 1998

Abstract. For Al containing compounds with different symmetry types of Al environment (from fourfold to 12-fold coordinated Al) it is revealed that Al K-XANES spectra are well reproduced by the XAFS code, based on the method of Hartree–Fock MT-potential generation, considering the photoelectron single-, double- and triple-scattering processes on approximately linear two- and three-atom chains, originated at the absorbing Al atom. The empirical 'selection rules' for choosing these chains are obtained and the origins of features in spectra are interpreted using the SELCOMP code. The proposed EXAFS-like approach for Al K-XANES description is applied also to explain the differences in Al K-XANES spectra, caused by the replacement of Fe atoms by Al atoms in goethite (α-FeOOH).

1. Introduction

X-ray absorption spectroscopy (XAS) is usually applied to local atomic structure determination through the analysis of the extended fine structure of the absorption spectrum (EXAFS). However, the EXAFS region of the spectrum often cannot be experimentally obtained due to either measurement conditions or the nature of compounds studied. For example, at the Al K edge, due to the kind of monochromator used, EXAFS oscillations are restricted to a short energy range and the only way to examine the structure of unknown compounds by XAS is to study the near edge spectrum region—XANES. On the other hand, XANES is very sensitive to the type of absorbing atom coordination [1] and contains more structural information than EXAFS. There are many publications devoted to XANES description in solids, but almost all of them use the full multiple scattering approach, in which the photoelectron scattering processes' contribution to the absorption cross-section is obtained through the system of algebraic equations within the Green's function method [2–5]. However, to solve the inverted problem—determination of interatomic distances, coordination numbers (CN) and bond-angles of atoms by XANES—preferable is the approach based on the consideration of photoelectron single, double and triple low-angle scattering processes on atomic chains, originated at the absorbing atom [6–8], named in the following the EXAFS-like approach. The aim of this paper is to prove that for compounds with different types of Al environment, the XANES spectra could be

‖ E-mail address: bugaev@rsu.rnd.runnet.ru; bugaev@phys.rnd.runnet.ru.

0953-8984/98/245463+11$19.50

described within the EXAFS-like approach, which provides the possibility to determine the local atomic structure in the vicinity of the absorbing atom using the extracted contribution to XANES from the photoelectron scattering on a single atomic chain, originated at the absorbing atom. For this purpose the Al K-XANES in Al metal—12-fold coordinated Al, berlinite ($AlPO_4$) and AlN—fourfold coordinated Al, K-alum ($KAl(SO_4)_2 12H_2O$), pyrophyllite ($Al_2(Si_4O_{10})(OH)_2$), diaspore (α-AlOOH) and kaolinite ($Al_2Si_2O_5(OH)_4$)—sixfold coordinated Al, were considered. The approach proposed is used also to explain the differences in Al K-XANES spectra caused by the replacement of Fe by Al atoms in goethite (α-FeOOH), and to find the possible atomic sites for such a replacement.

2. Experiment

Al K-XANES spectra were collected on the SA32 line at the LURE/Super-ACO facility (Orsay, France) using two α-quartz monochromator crystals ($10\bar{1}0$). The Super-ACO storage ring was operating at 800 MeV and 100–300 mA. The sample preparation consists of powder samples mounted directly on copper slides after dispersion in acetone and placement in the sample chamber under a vacuum of 10^{-5} Torr. Al K-XANES spectra were collected over a photon energy range of 1550–1600 eV in 0.2 eV steps. The x-ray beam is focused on the sample thanks to a toroidal mirror and the experimental energy resolution is of the order of 0.5 eV. More detailed information on sample preparation and spectrum measurements can be found in [9].

3. Method of calculation

To reveal the difference between the full multiple-scattering (MS) approach and the proposed one, the absorption cross-section of an atom in the compound must be written as:

$$\sigma(\varepsilon) = \sigma_{at}(\varepsilon)[1 + \chi(\varepsilon)] \tag{1}$$

where ε is the photoelectron energy started from the interstitial potential, named as muffin-tin (MT) zero, $\sigma_{at}(\varepsilon)$ is the absorption cross-section of the atom in the studied compound, obtained without regard for the neighbouring atom contribution and $\chi(\varepsilon)$ is the total contribution to $\sigma(\varepsilon)$ from all possible photoelectron scattering processes on pathways originated at the absorbing atom. Within the full MS approach, $\sigma(\varepsilon)$ can be calculated exactly, but when we are going to study the spectrum formation considering the different scattering processes on pathways or corresponding atomic chains, it is necessary to represent it as the row of terms:

$$\chi(\varepsilon) = \chi_{SS}(\varepsilon) + \sum_{i=1}^{\infty}[\chi_2^{(i)}(\varepsilon) + \chi_3^{(i)}(\varepsilon) + \chi_4^{(i)}(\varepsilon) + \cdots] \tag{2}$$

where $\chi_{SS}(\varepsilon)$ is the contribution of single-scattering (SS) processes on two-atom chains, and $\chi_2(\varepsilon)$, $\chi_3(\varepsilon)$, $\chi_4(\varepsilon)$, ... are respectively the double-, triple- and higher-order scattering terms on the ith chain, consisting of two or more atoms (see figure 1). The expressions for χ_{SS}, χ_2 and χ_3 obtained within the spherical wave formalism can be found in [10] and are realized in the XAFS code [7]. In several publications [7, 11, 12] it was shown that for some compounds, XANES can be described within the approximation which takes into account the SS-term of (2) and terms χ_2 and χ_3 from approximately linear three-atom chains chosen under the empirical selection rule. This selection rule was obtained through the fitting of theoretical spectrum to the experimental one, and depends upon the type of studied atomic structure and the types of scattering atom. It consists in the maximum value of scattering

pathway length (R_{max}) on atomic chains and in the minimum value of angle parameter $A = |\cos\alpha|$ for these chains (see figure 1). So the chains, considered when calculating XANES, must have their A values within $A_{min} \leqslant A \leqslant 1.0$, and their scattering pathway length must be $\leqslant R_{max}$. Under this approximation the expression (2) may be rewritten as:

$$\chi(\varepsilon) = \chi_{SS}(\varepsilon) + \sum_{i=1}^{p}[\chi_2^{(i)}(\varepsilon) + \chi_3^{(i)}(\varepsilon)] + S(\varepsilon) \tag{3}$$

where p is the number of three-atom chains, chosen under the empirical selection rule, and $S(\varepsilon)$ is the remaining sum over all other possible scattering processes. If the studied XANES can be reproduced within the used approach by the first and second terms of (3), then it means that $S(\varepsilon)$ is negligible. This is a nontrivial conclusion since calculations show that a lot of terms, presented in $S(\varepsilon)$, are not negligible themselves. Moreover, the convergence of terms in (2) under different photoelectron mean-free path values $\lambda(\varepsilon)$ in the near edge region, cannot be easily understood considering more terms of (2), and must be studied elsewhere. However, the preliminary analysis, carried out for different types of crystalline structure [7, 11, 12], shows that before the convergence takes place, there is a strong cancellation of terms, not included in the empirical selection rule. The cancellation probably occurs when these high-frequency terms are summarized with different random phases. In the following, the fitting procedure of the theoretical spectrum to the experimental one will be carried out using the SS-terms $\chi_{SS}(\varepsilon)$, and MS-terms $\chi_2(\varepsilon)$ and $\chi_3(\varepsilon)$ of (3).

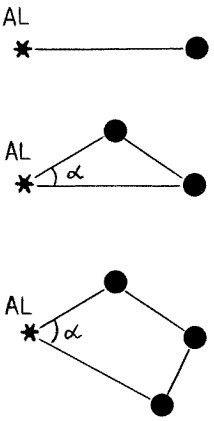

Figure 1. Schematic representation of two-, three- and four-atom chains, originated at the absorbing Al atom.

The phase shifts for photoelectron scattering on atoms in the studied compounds were calculated using the method of Hartree–Fock (HF) MT-potential generation [11, 13]. This method permits us to obtain theoretical XANES and EXAFS spectra systematically in agreement with the experimental ones [11–14]. With its help the high accuracy for structure parameters of first shell is obtained from EXAFS data analysis, using the calculated phase shifts and scattering amplitudes [15]. Within this method, the electronic configuration $Al(1s^1 2s^2 \ldots 3p^2)$ was used for the absorbing atom, in which the number of 3p electrons was increased by one to account for the 1s core hole screening. The value of nonphysical jump (δ) on the chosen MT-sphere radius (R_{mt}) of the absorbing Al atom was estimated [11]. For all neighbouring atoms, the ground state electronic configurations were used, and the radii of their MT-spheres were chosen so as to make equal the values of jumps on

each MT-sphere radius. According to the prescription of paper [11], the value of energy-independent interstitial potential ε_{mt} for the treated cluster was chosen then so as to suppress this potential jump value, i.e. $\varepsilon_{mt} = \delta$. The advantages of the used HF MT-potential model, compared to others are: (a) the simplicity of the potential generating procedure, which provides the energy independent interstitial potential value ε_{mt}, used then as the beginning of photoelectron energy or wave number; (b) it does not need any preliminary knowledge on the nearest shell distances or coordination numbers; (c) if necessary, the charges of atoms in the compound can be easily taken into account within this model [16].

For each compound the HF MT-potential was generated. The XAFS code was used then to calculate the amount of SS and MS contributions from photoelectron scattering on two- and three-atom chains, originated at the absorbing Al-atom. These chains were chosen under the initial conditions: $A_{min} = 0.8$, $R_{max} = 24$ Å, and corresponding SS- and MS-terms were used then by the SELCOMP code, which needs also the experimental spectrum of the compound studied. The SELCOMP code finds the best description of the experimental spectrum (maximum value of correlation coefficient) through the fitting procedure of theoretical spectrum to the experimental one. Within this fitting, the theoretical spectrum is obtained by (3), adding to SS-terms the MS-ones. The SELCOMP code outputs are the obtained theoretical spectrum of the compound and the selection rule (A_{min}, R_{max}) for atomic chains which must be taken into account to describe the experimental XANES. Besides, the SELCOMP code gives us the possibility to analyse the role of scattering processes on different atoms or atomic chains in XANES formation.

The photoelectron extrinsic losses were taken into account through the traditional exponential form $\exp(-R/\lambda(\varepsilon))$ [7] and intrinsic losses through the energy-dependent reduction factor $S_0^2(\varepsilon)$ [17]. The mean free path $\lambda(\varepsilon)$, as well as $S_0^2(\varepsilon)$, are usually not known exactly, especially for the near-edge region ($\leqslant$20 eV above the absorption threshold) of spectrum. However, the model calculations of XANES, carried out with 'reasonable' $\lambda(\varepsilon)$ values, do not change dramatically the obtained spectrum fine structure. Therefore the smooth energy dependences for $\lambda(\varepsilon)$ and $S_0^2(\varepsilon)$ in the near-edge energy region were chosen so as to adjust the envelope of the experimental spectrum.

4. Results and discussion

4.1. Al metal

In Al metal the absorbing Al atom is solely 12-fold coordinated by Al atoms with first shell radius $R_1 = 2.863$ Å. In figure 2(a) the experimental Al K-XANES spectrum [18] is compared with the theoretical one, obtained by SELCOMP. Calculations carried give the Al K-XANES in Al metal to be formed by SS-processes on five shells, nearest to the absorbing Al atom, and MS-processes on three linear three-atom chains within this cluster. The obtained results are summarized in the selection rule: $A_{min} = 1.0$ and $R_{max} = 13.2$ Å, justifying the validity of the EXAFS-like approach for XANES description in Al metal.

4.2. Fourfold coordinated Al

Berlinite, $AlPO_4$, has a distorted tetrahedral coordination of Al atoms with one aluminum site and point symmetry 2. The Al shift from the centre of the oxygen-tetrahedron results in the splitting of this tetrahedron into two subshells relative to the absorbing Al atom, with radii $R_1 = 1.732$ Å and $R_2 = 1.745$ Å [19]. The SELCOMP calculations of Al K-XANES show that, to obtain agreement with the experimental spectrum, one must consider

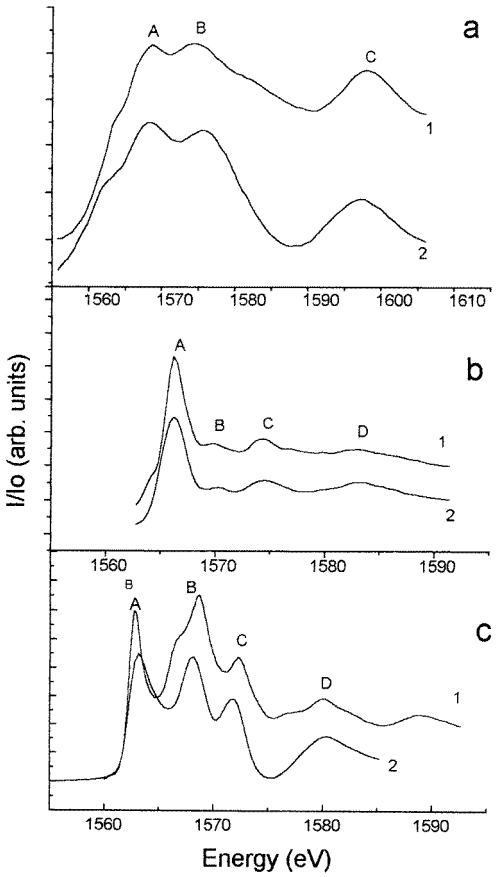

Figure 2. Experimental (curves 1) and theoretical (curves 2) Al K-XANES spectra of: (a) Al metal (CN = 12); (b) berlinite (CN = 4) and (c) AlN (CN = 4).

the photoelectron scattering processes on two- and three-atom chains, chosen under the selection rule: $A_{min} = 0.98$ (approximately linear chains, originated at the absorbing Al atom) and $R_{max} = 16.7$ Å. The last value could be treated as the diameter of the used cluster. In figure 2(b) the obtained theoretical Al K-XANES spectrum of berlinite is compared with the experimental one. As can be seen the spectrum is characterized by the presence of strong resonance A at 1566.8 eV and the following peaks B, C, D. The SELCOMP gives that the peaks A, B, D are formed mainly by the SS-processes within the used cluster, while the C-peak is formed by the MS-processes on chosen atomic chains. Analysing the effect of cluster size on the spectrum fine structure, we have found in agreement with [20] that the accounting for the scattering processes only on the nearest four oxygen atoms could not reproduce the spectrum structure, which is formed mainly by the photoelectron scattering on more distant shells with radii up to the cluster radius i.e. 8.35 Å.

AlN has a weekly distorted wurtzite-type structure in which Al is shifted from the centre of the N-tetrahedron. As a result this tetrahedron is split relative to the absorbing Al atom into two subshells with radii $R_1 = 1.889$ Å and $R_2 = 1.903$ Å [21]. Calculations and analysis of Al K-XANES in AlN carried out by SELCOMP show that the main features of the experimental spectrum presented in figure 2(c) are reproduced considering

SS- and MS-processes on two- and approximately linear three-atom chains, chosen under the selection rule: $A_{min} = 0.99$ and $R_{max} = 23.5$ Å. At the same time, the comparison of theoretical and experimental spectra in figure 2(c) shows that the fine structure on the left shoulders of peaks B and D is not reproduced in the theoretical spectrum calculated under the obtained selection rule. We have found that to reproduce it, the number of considered atomic chains must be increased.

4.3. Sixfold coordinated Al

Sixfold aluminum compounds studied are: K-alum, pyrophyllite, diaspore and kaolinite. The first three compounds are characterized by one octahedral aluminum site with point symmetry from $m3m$ in K-alum to 1 in pyrophyllite. In kaolinite the aluminum atoms are in two octahedral sites (point symmetry 1).

K-alum, $KAl(SO_4)_2 12H_2O$, has a non-distorted octahedral Al coordination with the first shell radius $R_1 = 1.908$ Å [22]. The experimental spectrum of K-alum represents two main peaks A and B (see figure 3(a)) at 1567.8 eV and 1572.2 eV respectively. The analysis of Al K XANES formation carried out by SELCOMP shows that to obtain agreement with the experimental spectrum, one must consider the scattering processes on two- and three-atom chains, chosen under the selection rule: $A_{min} = 1.0$ (only linear chains) and $R_{max} = 12.7$ Å. The theoretical Al K-XANES in K-alum, obtained under this selection rule, is compared with the experimental one in figure 3(a).

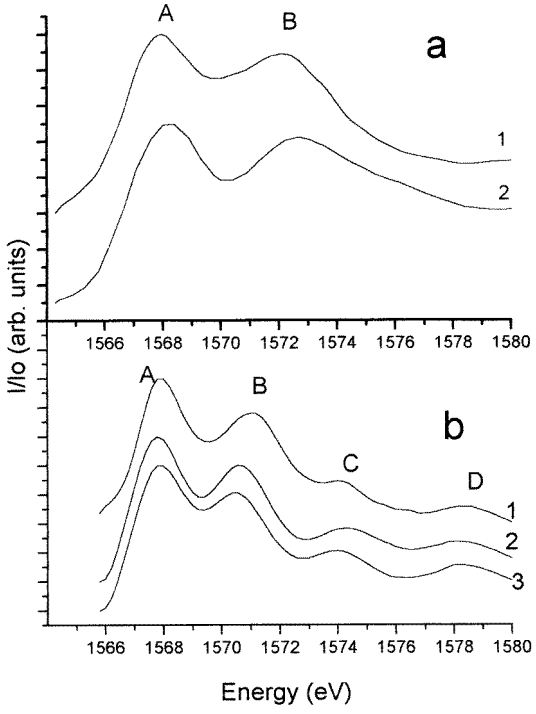

Figure 3. Experimental (curves 1) and theoretical (curves 2) Al K-XANES spectra of compounds with sixfold coordinated Al (CN = 6): (a) K-alum and (b) pyrophyllite. Curve 3 in (b) corresponds to a 'pure' oxygen environment of the absorbing Al atom.

Pyrophyllite, $Al_2(Si_4O_{10})(OH)_2$, has a distorted octahedral Al coordination with one Al site and Al–O distances for the nearest oxygens can be grouped in two sets at about 1.88 and 1.92 Å [23]. The experimental Al K-XANES—curve 1 in figure 3(b)—is characterized by two main peaks A at 1567.8 eV, B at 1571.2 eV and weak features C, D. SELCOMP calculations reproduce the peaks A and B with energy separation 3.0 eV and features C, D under the selection rule: $A_{min} = 0.97, R_{max} = 18.1$ Å. This theoretical spectrum is compared in figure 3(b) (curve 2) with the experimental one and with Al K-XANES, calculated under the same selection rule, but considering the scattering processes only on oxygen atoms ('pure' O environment of absorbing Al atom)—curve 3. Comparing curves in figure 3(b) one could find that Al K-XANES in pyrophyllite is formed mainly by SS- and MS-processes on two- and three-atom chains, which consist of the absorbing Al atom and O atoms, chosen under the obtained selection rule.

Diaspore, α-AlOOH, has a distorted octahedral coordination, resulting in four nearest oxygen shells with radii: $R_1 = 1.852$ Å (two atoms), $R_2 = 1.858$ Å (one atom), $R_3 = 1.975$ Å (two atoms), and $R_4 = 1.980$ Å (one atom) [24]. Experimental Al K-XANES of diaspore (curve 1 in figure 4), represents three main peaks A, B and C at energies 1567.4 eV, 1571.2 eV and 1587 eV respectively. The SELCOMP analysis gives that to describe experimental spectrum one must consider the SS- and MS-processes on approximately linear atomic chains, chosen under the selection rule: $A_{min} = 0.998$ and $R_{max} = 18.3$ Å. The comparison of the theoretical spectrum with the experimental one in figure 4 shows the agreement of their fine structures, except for the value of energy separation between peaks A and B, which is in theoretical one smaller by ∼0.5 eV, and the presence of an additional feature at 1576 eV, not observed in the experimental spectrum. However, the same discrepancies with the experiment occur for the spectrum calculated within the full MS approach [20], and therefore additional analysis of their origins is needed.

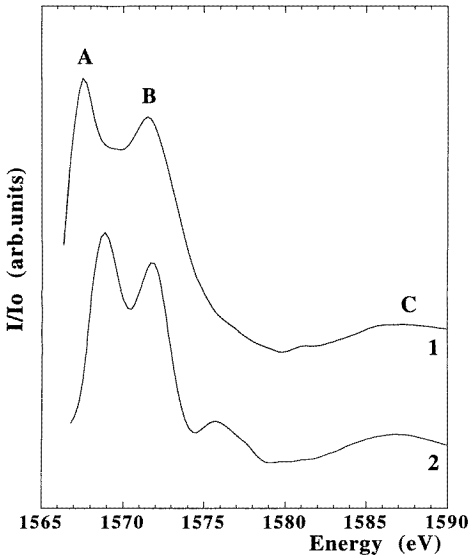

Figure 4. Experimental (curve 1) and theoretical (curve 2) Al K-XANES of diaspore (CN = 6).

In contrast to K-alum, pyrophyllite and diaspore, kaolinite—$Al_2Si_2O_5(OH)_4$—has two distorted octahedral aluminum sites [25], named in the following site 1 (with nearest

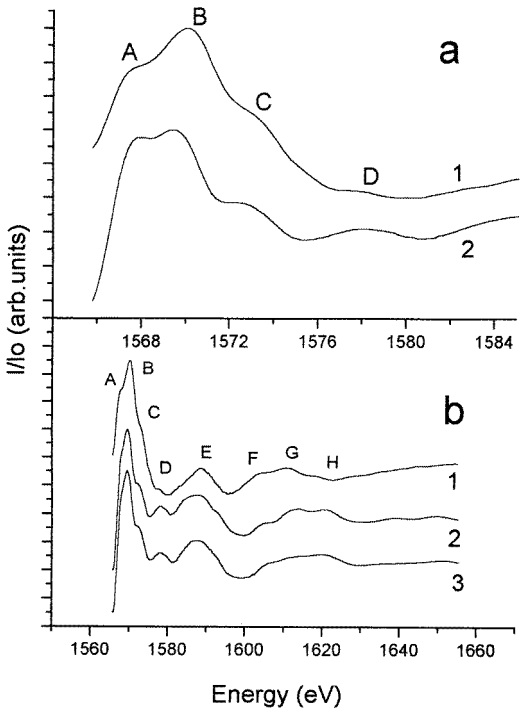

Figure 5. Experimental (curves 1) and theoretical (curves 2) K absorption spectra of Al in kaolinite (CN = 6): (a) XANES; (b) comparison in the extended energy-range. Curve 3 in (b) corresponds to a 'pure' oxygen environment of the absorbing Al atom.

oxygens at $R_1 = 1.880$ Å, $R_2 = 1.942$ Å) and site 2 (with oxygens at $R_1 = 1.894$ Å, $R_2 = 1.942$ Å). The experimental Al K-XANES of kaolinite—curve 1 in figure 5(a)—represents the two weakly separated peaks A (at 1568.2 eV) and B (at 1570.8 eV) and the extended fine structure. One more difference, comparing to the previous XANES for sixfold Al compounds, consists in the inversion of peaks A and B intensities $(I) : I_B > I_A$. The SELCOMP calculations for the two different Al sites give $\chi^{(1)}(\varepsilon)$ and $\chi^{(2)}(\varepsilon)$ functions, obtained under the same selection rule: $A_{min} = 0.97, R_{max} = 19.0$ Å, and the resulting theoretical Al K-XANES spectrum is obtained, summing the $\chi^{(1)}$ and $\chi^{(2)}$. Calculation results justify the energy separation between peaks A and B in kaolinite to be ~2.5 eV both in $\chi^{(1)}$ and $\chi^{(2)}$, in agreement with the experiment, which is by more 1 eV smaller than that for the minerals treated above in 4.3. Besides, the B-peak intensity in $\chi^{(2)}$ increases compared to $\chi^{(1)}$ and these two changes in the $\chi(\varepsilon)$ function, being multiplied by $\sigma_{at}(\varepsilon)$ in (1), lead to approximately equal intensities of peaks A and B ($I_A \approx I_B$) and their weak energy separation in the theoretical Al K XANES—curve 2 in figure 5(a). In figure 5(b) the experimental Al K XAS of kaolinite (curve 1) in the energy region up to 1660 eV is compared with the theoretical spectrum (curve 2) obtained within the used EXAFS-like approach and the theoretical spectrum calculated within the same approach but in the assumption of a 'pure' oxygen environment of the absorbing Al atom (curve 3). As can be seen, Al K-XANES of kaolinite is formed mainly by the photoelectron scattering on two- and three-atom chains, which consists of the absorbing Al atom and O atoms, chosen under the selection rule obtained by SELCOMP for the kaolinite structure.

4.4. Local Al environment in $Fe_{1-x}Al_xOOH$

The proposed approach was applied to explain the changes in Al K-XANES spectra, which occur under the replacement of Fe atoms by Al atoms in goethite (α-FeOOH). Goethite and diaspore have the same structure (space group *Pnma*) and a partial solid solution $Fe_{1-x}Al_xOOH$ (Al goethite) is known to exist between these two minerals. Up to 33 mol% of AlOOH can be substituted for Fe [26]. The Al K-XANES spectra of $Fe_{1-x}Al_xOOH$ for $x = 0.1$, 0.3, 0.33 (10, 30, 33 AlOOH mol% respectively) are compared in figure 6 taken from [9]. As can be seen, the significant difference between Al K-XANES spectra consists in the inversion of peak A and B intensities, which occurs with increasing AlOOH concentration from 30 to 33 AlOOH mol%. The increasing of AlOOH concentration leads also to an increasing energy separation between peaks A and B, from 3.2 eV in $Fe_{0.9}Al_{0.1}OOH$ to 3.8 eV (as for diaspore) in $Fe_{0.67}Al_{0.33}OOH$.

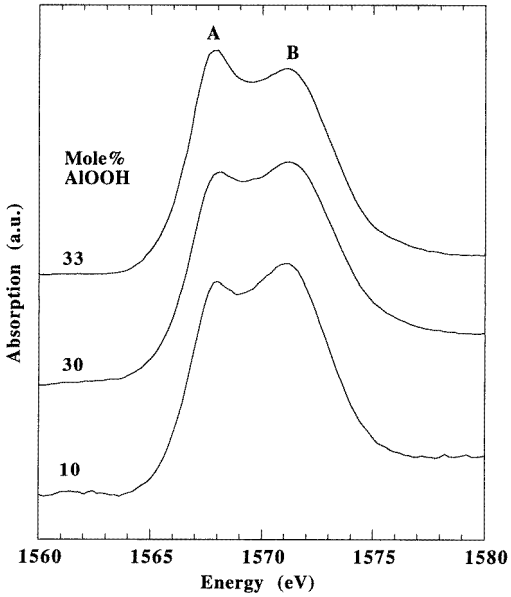

Figure 6. Experimental Al K-XANES spectra of goethite with different AlOOH concentrations [9]: 10, 30 and 33 mol%.

The SELCOMP calculations of Al K-XANES for one Al atom, surrounded by O and Fe atoms in goethite structure, show that the inverted intensities of peaks A and B ($I_A < I_B$) and energy separation of $\sim$3.0 eV between them are obtained under the selection rule: $A_{min} = 0.994$ and $R_{max} = 18.9$ Å. The corresponding theoretical spectrum for one Al in goethite is compared in figure 7 with the experimental Al K-XANES for $Fe_{0.9}Al_{0.1}OOH$. To make this comparison, we assume, in agreement with the experiment [9], that Al K-XANES spectra in goethite under low AlOOH concentrations ($\leqslant$15 mol%) are quite similar to each other. We have also calculated Al K-XANES for a model compound, consisted of an absorbing Al atom, surrounded by O and Al atoms only, in goethite structure, keeping the cell parameters of goethite. The comparison of the calculated spectrum with the experimental Al K-XANES of diaspore shows that the increasing energy separation between peaks A and B with increasing AlOOH concentration in $Fe_{1-x}Al_xOOH$ occurs mainly due to the decreasing of unit cell parameters, accompanying this substitution process.

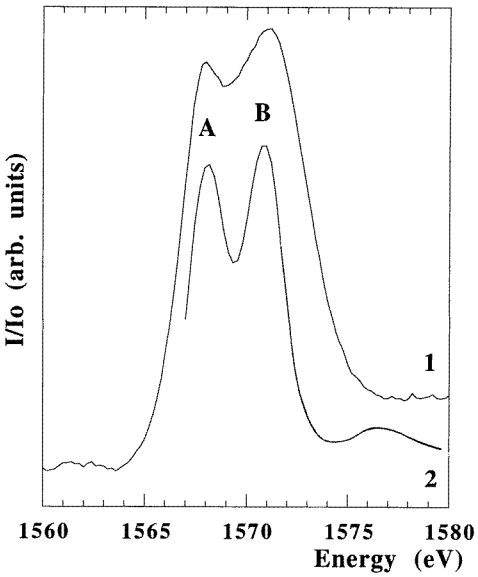

Figure 7. Experimental Al K-XANES of goethite with 10 mol% AlOOH concentration (curve 1) and theoretical Al K-XANES (curve 2), calculated for one absorbing Al atom, surrounded by O and Fe atoms in goethite structure.

The difference between the selection rules obtained for diaspore and Al goethite with 33 AlOOH mol%, can be used to find the possible sites in goethite structure for the replacement of Fe by Al atoms which lead to the inversion of peaks A and B intensities. From the point of view of photoelectron scattering description and the obtained selection rules, each site in the lattice can be considered as a 'pure' SS-site—S1—or as a mixed SS- and MS-site—S2. S2-sites belong to three-atom chains, chosen under the selection rule. The number of S2-sites included in the selection rules for diaspore and goethite structures are noted respectively as $(N)_{diasp}$ and $(N)_{goeth}$, where $(N)_{goeth} > (N)_{diasp}$, as can be seen from the selection rules. The SELCOMP analysis shows that the replacement of Fe atoms by Al atoms on S1-sites and on the $(N)_{diasp}$ number of sites S2 does not invert the intensities of peaks A and B, which explains the stability of spectrum structure with increasing AlOOH concentration in goethite up to 30 mol%. We can conclude therefore, that the inversion of peak A and B intensities when AlOOH concentration increases from 30 to 33 mol%, reflects the replacement of Fe atoms by Al atoms on $[(N)_{goeth} - (N)_{diasp}]$ number of S2-sites. These sites can be found using the SELCOMP output files, which gives the positions at 5.49 Å, 5.67 Å, etc, relative to the absorbing Al atom in the goethite structure.

5. Summary and conclusions

We have revealed that Al K-XANES of compounds with four-, six- and 12-fold coordinated Al atoms can be described through the EXAFS-like approach i.e. considering the photoelectron single-, double- and triple-scattering processes on two- and approximately linear three-atom chains, originated at the absorbing Al atom. The XANES spectra within this approach are obtained using the developed SELCOMP code, through the fitting of experimental spectrum by SS- and MS-terms, calculated with the help of the curved-wave

XAFS code [7], based on the method of HF MT-potential generation [11]. The proposed empirical 'selection rules' for choosing the atomic chains, which must be considered when calculating XANES, enable us to reveal the role of different environment atoms in Al K-XANES formation and to interpret the features in spectra. The analysis carried out gives, in contrast with the results of [27], that tetrahedrally and octahedrally coordinated aluminum, especially the distorted and undistorted Al sites, cannot be easily distinguished by the characteristic features in experimental XANES, without direct calculations of spectra for the proposed types of crystalline structure. The obtained results and the developed XAFS and SELCOMP codes permit us now to turn to the inverted problem—determination of local atomic structure in the distorted Al containing compounds, using their XANES.

Acknowledgment

This work was supported by the University Paris 7, grant 36MCF0227 (1997).

References

[1] Knapp G S, Veal B W, Pan H K and Klippert T 1982 *Solid State Commun.* **44** 1343–5
[2] Gurman S J, Binstead N and Ross I 1984 *J. Phys.: Condens. Matter* **17** 143–51
[3] Natoli C R, Misemer D K, Doniach S and Kutzler F W 1980 *Phys. Rev.* A **22** 1104-6
[4] Vedrinskii R V, Bugaev L A, Gegusin I I, Kraizman V L, Novakovich A A, Prosandeev S A, Ruus R, Maiste A and Elango M A 1982 *Solid State Commun.* **44** 1401–7
[5] Durham F J, Pendry J B and Hodges C H 1982 *Comput. Phys. Commun.* **25** 193–205
[6] Bunker G and Stern E A 1984 *Phys. Rev. Lett.* **52** 1990–3
[7] Vedrinskii R V, Bugaev L A and Levin I G 1988 *Phys. Status Solidi* b **150** 307–14
[8] Rehr J J, Albers R C and Zabinsky S I 1992 *Phys. Rev. Lett.* **69** 3397–400
[9] Ildefonse Ph, Cabaret D, Sainctavit Ph, Calas G, Flank A-M and Lagarde P 1998 *Phys. Chem. Miner.* **25** 112–21
[10] Bugaev L A, Vedrinskii R V and Levin I G 1989 *Physica* B **158** 378–82
[11] Bugaev L A, Vedrinskii R V, Levin I G and Airapetian V M 1991 *J. Phys.: Condens. Matter* **3** 8967–79
[12] Bugaev L A, Sokolenko A P, Cabaret D, Ildefonse Ph and Sainctavit Ph 1997 *J. Physique Coll.* IV **7** C2 141–2
[13] Vedrinskii R V, Bugaev L A and Airapetian V M 1991 *J. Phys. B: At. Mol. Opt. Phys.* **24** 1967–75
[14] Bugaev L A, Shuvaeva V A, Alekseenko I B, Zhuchkov K N and Husson E 1997 *J. Physique Coll.* IV **7** C2 179–81
[15] Vedrinskii R V, Bugaev L A and Levin I G 1989 *Physica* B **158** 421–4
[16] Bugaev L A and Vedrinskii R V 1985 *Phys. Status Solidi* **132** 459–64
[17] Rehr J J, Bardyszewski W and Hedin L 1997 *J. Physique Coll.* IV **7** C2 97–8
[18] Wong J, Rek Z U, Rowen M, Tanaka T, Schafers F, Muller B, George G, Pickering I J, Via G, DeVries B, Brown G E and Froba M 1995 *Physica* B **208/209** 220–2
[19] Schwarzenbach von D 1966 *Z. Kristallogr.* **123** 161–85
[20] Cabaret D, Sainctavit Ph, Ildefonse Ph and Flank A-M 1996 *J. Phys.: Condens. Matter* **8** 3691–704
[21] Schulz H and Thiemann K H 1977 *Solid State Commun.* **23** 815–9
[22] Larson A C and Cromer D T 1967 *Acta Crystallogr.* **22** 793–800
[23] Lee J H and Gugggenheim S 1981 *Am. Mineral.* **66** 350–7
[24] Busing W R and Levy H A 1958 *Acta Crystllogr.* **11** 798–803
[25] Bish D L and Von Dreele R B 1989 *Clays Clay Miner.* **37** 289–96
[26] Fitzpatrick R W and Schwertmann U 1982 *Geoderma* **27** 335–47
[27] van Bokhoven J A, Sambe H, Koningsberger D C and Ramaker D E 1997 *J. Physique Coll.* IV **7** C2 835–40